stellarator news

Published by Fusion Energy Division, Oak Ridge National Laboratory
Building 9201-2 P.O. Box 2009 Oak Ridge, TN 37831-8071, USA

Editor: James A. Rome Issue 58 July 1998
E-Mail: jar@ornl.gov Phone (423) 574-1306 Fax: (423) 576-3647
On the Web at *http://www.ornl.gov/fed/stelnews*

Magnetic flux mapping in LHD

The first plasma in the Large Helical Device (LHD) was produced on March 31, 1998; the initial plasma experiments then continued until May 13. In this first phase of the experiment, LHD was operated with a toroidal magnetic field B_0 of 1.5 T and plasmas were produced and heated with second harmonic electron cyclotron heating (ECH). The maximum total ECH power was about 350 kW at frequencies of 84.0 and 82.6 GHz. The plasma quality improved with wall conditioning, and it was shown in the last stage of the initial plasma experiments that the maximum electron temperature is about 1.5 keV and the maximum flat-top density is about 1.0×10^{19} m^{-3}. A preliminary analysis of the energy confinement time indicates that it appears to agree with the value estimated from the empirical scaling law.

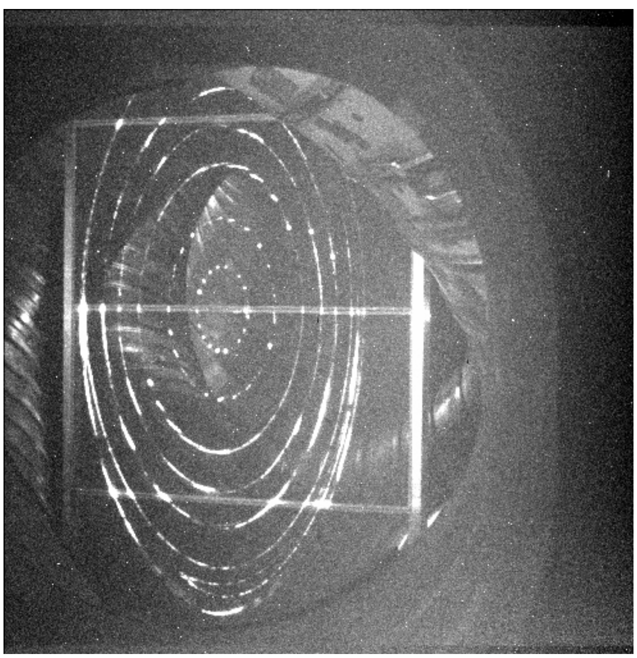

Fig. 1. Magnetic surfaces in LHD at B_0 = 0.0875 T, measured using the fluorescent mesh method.

In this issue . . .

After the initial plasma experiments, magnetic flux mapping studies were performed during steady-state operation at reduced B_0, up to 0.25 T. The mapping was carried out by the fluorescent method, using an electron gun with a LaB_6 cathode and a fluorescent mesh that emits light when the electron beam collides with it. The diameter of the electron beam was limited to < 3 mm by an aperture. The 1 × 2 m fluorescent mesh was situated at the toroidal plane where the cross sections of magnetic surfaces are elongated vertically. The magnetic surfaces were measured by taking pictures of the fluorescent mesh while changing the radial position of the electron gun. The pictures were taken with an intensified charge-coupled device (CCD) camera, whose line of sight was along the centerline of a tangential port for the neutral beam injection, and the angle between the line of sight and fluorescent mesh was 65°.

Clear pictures of the magnetic surfaces were obtained (Fig. 1), revealing closed, nested magnetic surfaces in good agreement with calculations, as can be seen in Fig. 2. The ability to create this accurate magnetic configuration is a prerequisite to the successful start-up of the LHD experiment. The rotational transform and magnetic shear are still being analyzed through comparisons of experiment and calculation.

Figure 1 shows also the existence of a clear $m/n = 1/1$ island. This island is considered to be formed by the earth's magnetic field because the LHD magnetic field was so low when the mapping was performed. Although only the $m/n = 1/1$ island is depicted in Fig. 1, very small $m/n = 2/1$ islands could be also observed experimentally. The calculation depicted in Fig. 2 takes into account the earth's magnetic field and hence demonstrates that the $m/n = 1/1$ and 2/1 islands could be formed by terrestrial magnetism at this low magnetic field. The calculated poloidal phases and maximum widths of the islands agree well with those of the experimental results; furthermore, the maximum width of the $m/n = 1/1$ island was reduced by a factor of about 1.3 when the mapping was performed at $B_0 = 0.25$ T, from that obtained at $B_0 = 0.0875$ T. Thus it is concluded that the observed islands are formed mainly by the earth's magnetic field. This will be shown more clearly in the second campaign of the LHD experiment, during which magnetic flux mapping studies will be performed at $B_0 = 1.5$ T. Even at this stage of the magnetic flux mapping studies, however, it is suggested that the accuracy of LHD, especially, with regard to the helical and poloidal coils, including their alignment, exceeds the required value for LHD, because the measured maximum island width of 8.9 cm at $B_0 = 0.25$ T is larger than the predicted maximum island width of 6 cm (which was calculated taking into account error fields caused by the permissible inaccuracy of these coils) by a factor of only about 1.5. Thus at the operating field of 1.5 T or 3.0 T, the island width will be significantly reduced.

The initial successful results of the magnetic flux mapping studies provide new hope and encouragement to the LHD experiment.

Akio Komori for the LHD Team
National Institute for Fusion Science
Toki 509-5292, Japan
E-mail: komori@LHD.nifs.ac.jp

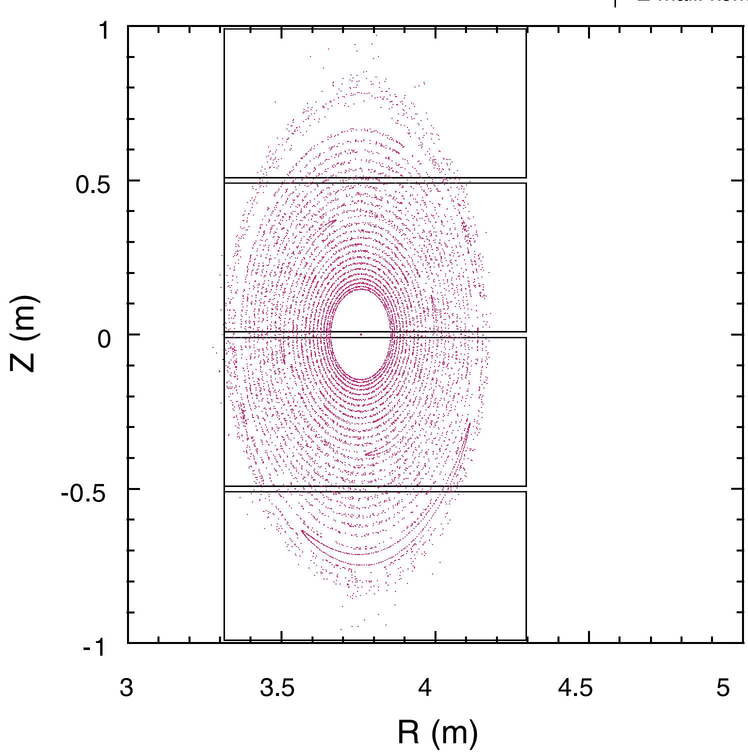

Fig. 2. Calculated magnetic surfaces in LHD at $B_0 = 0.0875$ T. The earth's magnetic field is taken into account. These should be compared to the experimentally-measured surfaces in Fig. 1.

Dynamics of the high ion temperature mode in CHS

Characteristics of high-T_i mode discharges

The high ion temperature T_i mode [1] is one of several improved modes in stellarators [2]. Recently, similar high-T_i mode discharges have been observed for neutral beam heated plasmas by turning off the gas puff at the onset of neutral beam injection (NBI) in the Compact Helical System (CHS) heliotron/torsatron.

Figure 1 shows profiles of T_i measured with charge-exchange spectroscopy (CXS) [3] for discharges without a gas puff (high-T_i mode) and with a gas puff (L-mode) in CHS. The target plasma is produced by a pulse of electron cyclotron resonance heating (ECRH) that produces a target plasma, and then a neutral beam is injected for 40–140 ms. The helical magnetic field is 1.76 T. While the electron density n_e increases with time because of gas puffing, T_i is almost constant in L-mode discharges. However, when the gas puff is turned off at the onset of NBI, both the central electron density, $n_e(0)$, and the central ion temperature, $T_i(0)$, increase in time and $T_i(0)$ reaches 0.7–0.8 keV. The transition between the high-T_i mode and the L-mode is sensitive to the ratio of beam fueling to gas puff fueling, and a small gas puff or high wall recycling will prevent the discharge from entering the high-T_i mode.

The absolute value of $n_e(0)$ in the high-T_i mode is similar to that in the early phase of an L-mode discharge. For example, $n_e(0)$ at t = 70 ms in the L-mode discharge is almost identical to the $n_e(0)$ at t = 90 ms in the high-T_i mode discharge in CHS. On the other hand, clear differences are observed between the n_e profiles for high-T_i mode discharges and those for L-mode discharges. In high-T_i mode discharges, the electron density profile is peaked (~1.5), while it is flat (~1.0) in the L-mode during gas puffing.

Transition from L-mode to the high-T_i mode

Figure 2(a) shows $T_i(0)$ as a function of NBI power in CHS. The central electron temperature increases gradually, proportional to $P^{0.35}$, as the NBI power is increased. However, the central ion temperature increases sharply at the critical NBI power of 0.7 MW. This sharp increase in ion temperature indicates the transition from L-mode to high-T_i mode. Since the coinjected NBI power in CHS is 0.7–0.8 MW, which is slightly higher than the critical value, a slight increase in the electron density by gas puffing prevents the discharge from making the transition from L-mode to high-T_i mode. Therefore, there is an upper limit on electron density for the high-T_i mode transition with a fixed NBI power, as seen in Fig. 2(b). In the low density regime (t = 70 and 90 ms), $T_i(0)$ drops sharply at $n_e(0)$ =

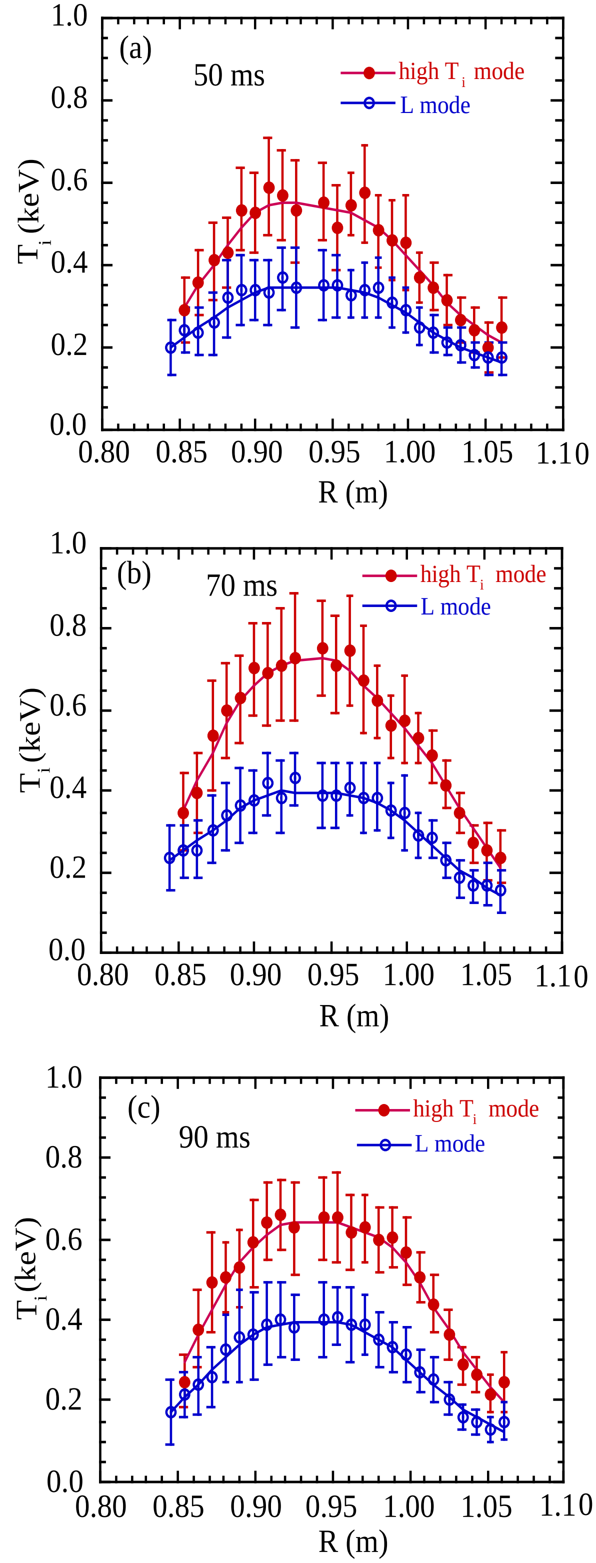

Fig.1 Radial profiles of ion temperature for L-mode and high-T_i mode discharges in CHS.

$1.4 \times 10^{19} m^{-3}$ (t = 70 ms) and $n_e(0) = 2.2 \times 10^{19} m^{-3}$ (t = 90 ms), indicating the upper limit for the high-T_i mode. The upper limit of the electron density for the high-T_i mode increases as the peaking factor of electron density is increased (1.5 at t = 70 ms → 1.8 at t = 90 ms). No sharp drop is observed at t = 110 ms because the electron density exceeds the upper limit for the high-T_i mode and the plasma is in the L-mode. When recycling is high due to poor wall conditions, the central electron density increases without a gas puff and the density peaking factor is low (< 1), so the plasma is always in the L-mode. To achieve a high T_i-mode discharge, the peaking factor should increase as the central electron density increases. Therefore central fueling by neutral beams is the key to achieving the high-T_i mode in CHS.

K. Ida and the CHS Group
National Institute for Fusion Science
Oroshi-cho, Toki-shi, Gifu, 509-5292, Japan

References

[1] K. Ida et al., Phys. Rev. Lett. **76**, 1268 (1996).

[2] A. Iiyoshi, in Fusion Energy (Proc. 16th Int. Conf. Fusion Energy, Montreal, 1996), IAEA, Vienna, Vol. 1, 113 (1997).

[3] K. Ida and S. Hidekuma, Rev. Sci. Instrum. **60**, 867 (1989).

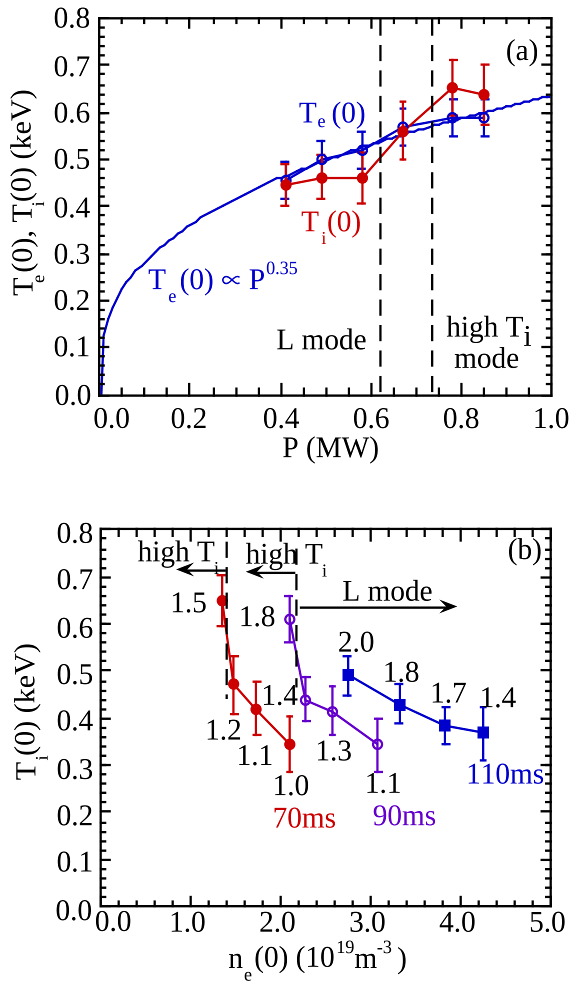

Fig. 2. (a) Central ion and electron temperatures as a function of NBI power. (b) Central ion temperature as a function of central electron density. The parameter on these curves is the density peaking factor.

First plasmas in the TJ-II Flexible Heliac

Introduction

TJ-II is a low magnetic shear stellarator of the Heliac type with an average major radius of 1.5 m and an average minor radius ~ 0.22 m. The magnetic field (B_0 = 1 T) is generated by a system of poloidal, toroidal, and vertical field coils. The main characteristics of TJ-II are (a) strong helical variation of its magnetic axis; (b) very favorable MHD characteristics with potential for high-beta operation; (c) flexibility in operation (the rotational transform can be varied over a wide range); and (d) bean-shaped plasma cross section [1].

The existence of closed, nested magnetic surfaces, in good agreement with the calculated ones, has been demonstrated in TJ-II by means of magnetic surface measurements carried out at low magnetic field [2, 3]. A powerful data acquisition system [4] is in operation to handle the large amount of data (~125 Mbytes/discharge) generated by the set of plasma diagnostics installed in the device [5]. The physics program of the TJ-II stellarator is focused on transport studies in low-collisionality plasmas, operational limits in high-beta plasmas, and studies of confinement optimization and its relationship with the radial electric field.

First results

The first TJ-II plasmas were obtained using one gyrotron (f = 53.2 GHz, P_{ECRH} ~ 250 kW) with a pulse length of Δt ~ 80–200 ms. Electron cyclotron resonance heating (ECRH) power is launched into TJ-II plasmas through a boron nitride window mounted on the bottom port at the toroidal angle ϕ = 25°, and perpendicular to the TJ-II magnetic field as an extraordinary wave [6, 7]. A set of receiving antennas has been installed along the TJ-II vessel in order to measure the multipass absorption. The measurements show that the residual microwave power, not directly absorbed by the plasma bulk, is absorbed after a few passes through the plasma column. This is in agreement with the extensive linear ray tracing calculations carried out to analyze the performance of the ECRH system in TJ-II [8, 9].

Prior to experiments, vacuum levels of ~ 1×10^{-7} mbar are achieved using a set of turbomolecular pumps whose total pumping speed is ~4000 L/s [10]. Room-temperature glow discharge cleaning with helium has been used for the conditioning of the stainless steel wall in the initial phase.

Five magnetic configurations were studied. Their parameters are shown in Table I. Two mobile limiters in TJ-II [11] make it possible to reduce the interaction between the plasma and vessel when required. A set of Langmuir probes and thermoresistors are embedded in the limiters to enable characterization of the scrape-off layer (SOL) region. Measurements with probes installed in the limiters and with fast movable probes show a good agreement (within ±0.5 cm) with the location of the last closed flux surface (LCFS) as computed from equilibrium codes and the confinement plasma radius (defined as the point where the electric field changes direction from positive (radially outwards) to negative. When magnetic islands are present in the plasma boundary region, a flattening in the edge profiles (i.e., in the ion saturation current and floating potential) has been observed. This is interpreted in terms of the influence of magnetic islands (8/5) on plasma profiles [12].

The typical time evolution of ECRH discharges is shown in Fig. 1 for the magnetic configurations having central rotational transform $\iota(0)$ ~ 1.51. Good conditions for preionization and plasma start-up by ECRH were achieved by injecting hydrogen several tens of milliseconds before the gyrotron pulse. Typical pressures are in the 10^{-5} mbar range, in agreement with particle balance; delays between the density build-up and the gyrotron pulse are typically a few milliseconds. Quasi-stationary discharges with ECRH lasting up to 200 ms were obtained. The plateau has an average electron density $\overline{n}_e$ ~ 0.5×10^{19} m^{-3} and central (ECE) electron temperatures are in the range T_e ~ 0.4 – 0.8 keV. The edge temperature is in the range $T_e(a)$ ~ 10–20 eV. The H_α signal decreases at the beginning of the plasma discharge whereas impurity monitors

Table I.
TJ-II configuration characteristics. R_0 and R_b are the mod(B) ripple at the magnetic axis and at the boundary, respectively.

Name	ι_0	ι_b	Well (%)	Volume (m^3)	R_0 (%)	R_b (%)
38_38_37	1.50	1.62	2.6	0.337	3.0	18.4
46_46_43	1.60	1.73	4.0	0.560	2.3	24.2
100_32_60	1.42	1.52	2.2	0.934	1.5	32.0
100_40_63	1.51	1.61	2.3	1.065	1.7	35.8
100_50_65	1.61	1.73	2.7	1.260	2.4	40.7

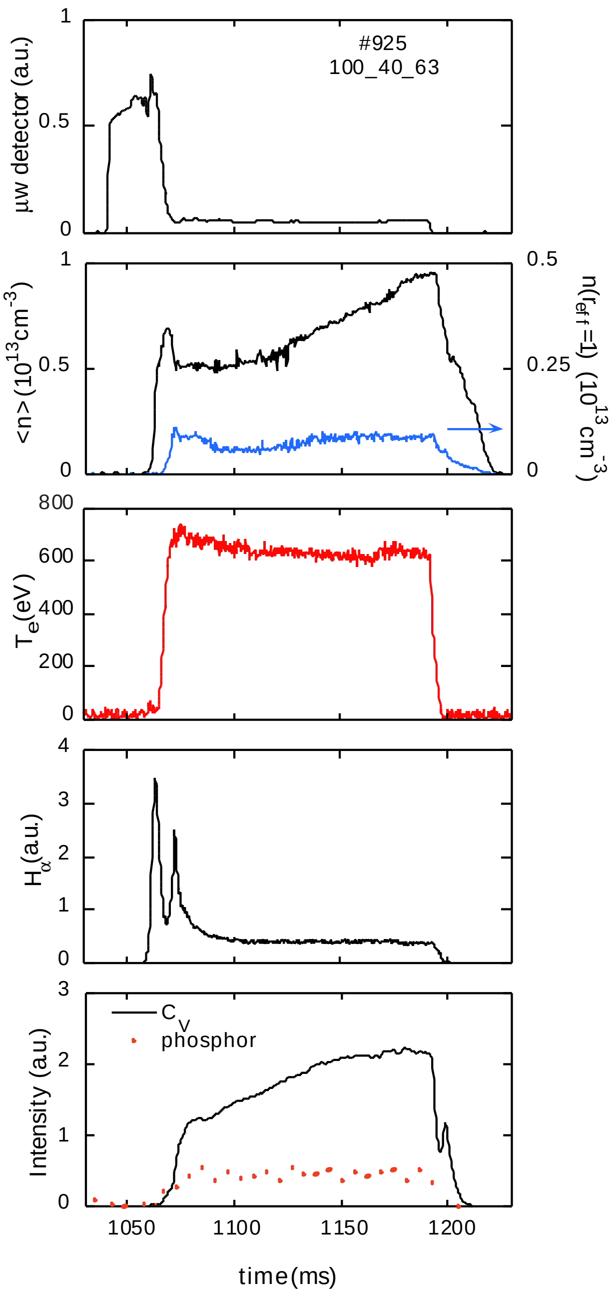

Fig. 1. The time evolution of plasma parameters with ɨ(0) ~ 1.51.

(i.e., carbon V) increase later. The fast decay of the H_α signal is consistent with the low recycling expected for helium-conditioned metallic walls. The constant electron density at longer times implies the presence of impurities as fueling species. Results for different configurations indicate an impurity dilution effect as the ratio of plasma volume to plasma-surface interaction increases [12]. In configurations with the largest volumes ($V \sim 1.2\ m^3$), plasma densities up to the cut-off density ($n_e(0) = 1.75 \times 10^{19}\ m^{-3}$) have been obtained with appropriate gas puffing during the plasma discharge. Plasma currents in the range of $I \sim 0.5$ kA have been measured, and appear to depend on the location of the plasma resonance (on/off-axis heating) consistent with electron cyclotron current drive (ECCD) calculations.

Global confinement properties have been found to be strongly dependent on plasma volume. Figure 2 shows stored plasma energy vs plasma volume. The stored energy increases from 200 J in the smallest plasma configuration ($V \sim 0.34\ m^3$) to above 1 kJ in the plasma configuration with $V \sim 1.2\ m^3$. In the largest plasma configurations, which have a line-averaged density $n_e \sim 0.5 \times 10^{19}\ m^{-3}$, the measured stored plasma energy W is ~1 kJ and the global energy confinement time $\tau_{E*} = W/P_{ECRH} \sim$ 4 ms.

Conclusions

The first plasmas of the TJ-II stellarator have been successfully achieved using a 53.2-GHz gyrotron with ECR heating ($P_{ECRH} \sim 250$ kW). Quasi-stationary discharges lasting up to 200 ms have been obtained with central electron temperatures from 400 to 800 eV, plasma densities $\overline{n_e} \sim (0.5–1) \times 10^{19}\ m^{-3}$, stored energies in the range 0.2–1 kJ and global energy confinement times of up to 4 ms. As

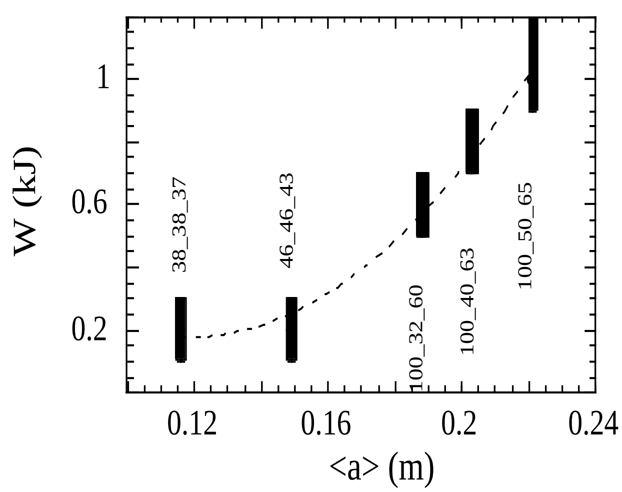

Fig. 2. Stored energy vs plasma volume for the shots in Table I.

expected in TJ-II, the plasma-wall interaction shows very distinctive features that play an important role in attaining the nominal flexibility range of the machine. An intense program in first wall conditioning is under development to control the influence of neutral particles and radiation on plasma properties.

References

[1] C. Alejaldre et al., Fusion Technol. **17**, 131 (1990).

[2] E. Ascasibar et al., J. Plasma Fusion Res. Series 1, 183 (1998).

[3] E. Ascasibar et al., Stellarator News (1998).

[4] J. Vega, C. Crémy, E. Sánchez, A. Portas, Fusion Eng. Des. (in press).

[5] J. Sánchez et al., J. Plasma Fusion Res. Series 1 (1998).

[6] R. Martin et al., Proc. 17th Symp. Fus. Techhnol., Rome, Italy, (1992) p. 897.

[7] M. Sorolla, et al., Int. J. Infrared Millimeter Waves **18**, 1161 (1997).

[8] F. Castejón, C. Alejaldre, and J. A. Coarasa, Phys. Fluids B **4**, 3689 (1992).

[9] V. Tribaldos, J.A. Jiménez, J. Guasp, and B. Ph. van Milligen, Plasma Phys. Controlled Fusion (1998) (in press).

[10] F. L. Tabarés et al.,Vacuum **45**, 1059 (1994).

[11] E. de la Cal et al., the 13th Plasma Surface Interactions Conference, San Diego, 1998, proceedings to be published in J. Nucl. Mater.

[12] TJ-II Team, in Proc. 25th EPS Conference, Prague, 1998.

Carlos Alejaldre for the TJ-II Team*
Asociación Euratom-CIEMAT para Fusión
Av. Complutense nº22
28040 MADRID
Phone: +34-1-346.6159
Fax: +34-1-346.6124

*C. Alejaldre, J. Alonso, L. Almoguera, E. Ascasíbar, A. Baciero, R. Balbín, M. Blaumoser, J. Botija, B. Brañas, E. de la Cal, A. Cappa, R. Carrasco, F. Castejón, J. R. Cepero, C. Cremy, J. Doncel, C. Dulya, T. Estrada, A. Fernández, M. Francés, C. Fuentes, A. García, I. García-Cortés, J. Guasp, J. Herranz, C. Hidalgo, J. A. Jiménez, I. Kirpitchev, V. Krivenski, I. Labrador, F. Lapayese, K. Likin, M. Liniers, A. López-Fraguas, A. López-Sánchez, E. de la Luna, R. Martín, A. Martínez, M. Medrano, P. Méndez, K. McCarthy, F. Medina, B. van Milligen, M. Ochando, L. Pacios, I. Pastor, M.A. Pedrosa, A. de la Peña, A. Portas, J. Qin, L. Rodríguez-Rodrigo, A. Salas, E. Sánchez, J. Sánchez, F. Tabarés, D. Tafalla, V. Tribaldos, J. Vega and B. Zurro.
Asociación Euratom-CIEMAT, 28040 Madrid, Spain

D. Akulina, O.I. Fedyanin, S. Grebenshchicov, N. Kharchev, A. Meshcheryakov
General Physics Institute, Moscow, Russia

R. Barth. G. van Dijk, H. van der Meiden
FOM-Instituut voor Plasmafysica, Rijnhuizen, The Netherlands

S. Petrov
Ioffe Physical Technical Institute, St. Petersburg, Russia

H-1 Heliac upgrade status

The H-1 flexible heliac project became an Australian Major National Research Facility (MNRF) in May 1997 with the signing of a contract between the Australian National University (ANU) and the Australian Department of Industry, Science and Tourism. This contract provides capital funding of $8.7 M (Australian) over five years to support increasing the magnetic field, heating power, and diagnostic capabilities.

The first stage of the upgrade process is now under way. The largest part of this project is to increase the magnetic field of the H-1 device (major radius of 1 m, plasma minor radius of 0.15–0.20 m) from its present operating value of 0.2 T to its design value of 1 T. This requires the addition of a power supply capable of providing 14 kA at 1 kV for a flat-top of 0.5 s at full power.

In late 1997, power supply design specifications were prepared by a team from ANU and Walsh & Associates Consulting Engineers in Sydney. After a competitive tender, contracts were awarded to ABB-Melbourne for the dc-dc converter and regulator (the largest component) and system integration, to TMC Ltd. of Melbourne for the transformer, to CEGELEC of Sydney for the ac-dc converter, and to HOLEC Engineering of Sydney for the high-voltage switchboard. These subsystems are now in detailed design, with component testing and installation scheduled for October–December 1998 and first operation for early 1999.

In parallel, substantial modifications to the experimental hall and adjoining service areas have been carried out. Pearson & Sullivan Pty. Ltd. of Canberra are responsible for the building modifications, and KONE, Ltd. of Sydney have installed a new overhead crane.

The upgrade of the H-1 heating is also progressing. Components for the waveguide line connecting the 200-kW, 28-GHz, Kyoto/NIFS gyrotron to H-1 have been fabricated and delivered by General Atomics (San Diego), and the gyrotron itself is having its output window upgraded by CPI in California. A 250-kW, 4- to 26-MHz transmitter for ion cyclotron resonant frequency heating (ICRF) was acquired from Radio Australia. It was dismantled and transported from Western Australia by Telstra and is being adapted and installed in the H-1 area by British Aerospace–Adelaide and Wilson Transformers of Melbourne.

H-1 will resume physics operation for a short period at low field in August–September 1998 and then will be shut down for final installation and testing of magnetic field power supply and heating system components October 1998 through January 1999.

Jeffrey Harris
Plasma Research Laboratory
Research School of Physical Sciences & Engineering
Institute of Advanced Study
The Australian National University
Canberra ACT 0200 AUSTRALIA
E-mail: Jeffrey.Harris@anu.edu.au

U.S. stellarator “proof-of-principle” proposal review

The U.S. stellarator community is proposing a “proof-of-principle” (PoP) program to develop the knowledge base on compact, high-beta, good-confinement stellarators that would allow a later decision on a compact stellarator that allows extrapolation to burning plasma conditions. The proposed program is based on development of hybrid magnetic configurations that combine the best features of stellarators (external control; immunity to disruptions; and no need for current drive, feedback stabilization, rotation drive, or a close conducting wall) and advanced tokamaks (compact, high beta, and good confinement). The stellarator proposal was reviewed by the U.S. Department of Energy (DOE) in June along with proposals for PoP programs in the reversed-field pinch and magnetized target fusion areas. The report of the review committee is expected shortly. Both this proposal and the “U.S. Stellarator Program Plan” are on the *Stellarator News* web site.

The proposed program is based on two promising transport optimization strategies for compact stellarators (with plasma aspect ratio A = 2–4): quasiaxisymmetry (QA) and quasiomnigeneity (QO). Quasisymmetric stellarators conserve a component of the canonical momentum (as do tokamaks) and have neoclassical transport properties that are tokamak-like. The Helically Symmetric Stellarator (HSX) at the University of Wisconsin will be the first experimental test and exploration of quasisymmetry, specifically, quasihelicity.

QA stellarators can have aspect ratios and bootstrap currents typical of tokamaks, so they resemble tokamak-stellarator hybrids. Like tokamaks, they can have a deep magnetic well and high beta limits for ballooning, even at a low aspect ratio. Although the last closed flux surface appears nonaxisymmetric in real space, the Fourier spectrum of $|\boldsymbol{B}|$ in magnetic coordinates (on which the particle drift orbits and neoclassical transport depend) has a dominant axisymmetric component with nonaxisymmetric components of only a few percent at the plasma edge.

The QO concept (1) reduces neoclassical losses by approximately aligning the collisionless trapped particle drift orbits with the magnetic surfaces and (2) provides a larger fraction of the rotational transform by external coils, reducing the fraction of the rotational transform that is created by the bootstrap current. This may ease startup, reduce the sensitivity of the equilibrium to changes in the bootstrap current, and reduce susceptibility to disruptions. The variation of the field strength within a magnetic surface can be more complicated than in quasisymmetric configurations since no particular symmetry is imposed. The large nonaxisymmetric terms in the $|\boldsymbol{B}|$ spectrum and the lower fraction of bootstrap current distinguish QO stellarators from QA stellarators.

Both the QA and QO concepts make use of the bootstrap current, but to different degrees, to create a configuration with A = 2–4 and volume-average beta ≥ 5% (the value projected for the advanced ARIES-RS tokamak reactor). Both look attractive for compact stellarator reactors, and each has distinct complementary advantages. Both must be developed experimentally to establish the needed scientific base for the program’s ultimate success. A determination of the optimum strategy to pursue is one of the U.S. stellarator program’s goals. The proposed program consists of the following elements:

- A new PoP facility, the National Compact Stellarator Experiment (NCSX)
- A new concept exploration experiment, the Quasi-Omnigeneous Stellarator (QOS)
- The existing HSX and a modification of the Compact Auburn Torsatron (CAT)
- Stellarator theory focusing on concept optimization and key stellarator physics issues
- Collaboration with the international stellarator program in specific areas
- System studies to guide concept optimization tradeoffs

The PoP program elements cross-link with one another to provide a well-integrated program.

The NCSX facility would be the focus of the PoP program. It would be reconfigurable to ensure that experimental tests of the new developments arising from the total stellarator program can be conducted expeditiously. In order to minimize cost, it is planned to construct the NCSX facility by modifying an existing device, the PBX-M tokamak, and using its supporting infrastructure. The QA concept is probably somewhat more compatible with the PBX-M constraints, so it has been chosen as the initial PoP configuration. The QOS experiment is proposed to test the basic principles of the complementary QO optimization strategy and to provide information needed for the design of the second coil configuration to be tested in the NCSX facility.

J. F. Lyon
Oak Ridge National Laboratory
Oak Ridge, TN 37831-8072
Phone: (423) 574-1179
E-mail: lyonjf@ornl.gov